Journal of Agricultural Machinery
Vol. 11, No. 1, Spring- Summer 2021, p. 55-70

نشریه ماشین‌های کشاورزی
جلد ۱۱، شماره ۱، نیمسال اول ۱۴۰۰، ص ۷۰-۵۵

Full Research Paper

Effect of Pomegranate Seed Oil Encapsulated in Chitosan-capric Acid Nanogels Incorporating Thyme Essential Oil on Physicomechanical and Structural Properties of Jelly Candy

H. Mirzaee Moghaddam[1*], A. Rajaei[1]

Received: 01-01-2020
Accepted: 23-05-2020

Abstract

Pomegranate seed oil (PSO) is a well-known source of valuable compounds. The aim of this study was to investigate physicomechanical and structural properties of jelly candy enriched with PSO encapsulated in chitosan (CS)-capric acid (CA) nanogel incorporating thyme essentioal oil (TEO). For this purpose, initially the CS-CA nanogels were produced by creating amide bondes between CS and CA, which Scanning Electron Microscope (SEM) image showed the spherical form of CS-CA nanogels. Then, PSO-in-water Pickering emulsions were stabilized with the CS-CA nanogels as well as the CS-CA nanogels incorporating TEO. The results showed that the presence of TEO in the nanogel structure caused smaller oil droplets. Then, Pickering emulsions were used in the formulation of jelly candy and subsequently the microscopic structure, texture profile analysis (TPA) and color indexes of jelly candies were studied. The use of PSO in the encapsulated form reduced the separation of the PSO from the texture of the jelly candy. The results of TPA showed that although the samples containing PSO in the encapsulated form had lower hardness (156.6-173.4 N), gumminess (202.2-262.1 N), cohesiveness (1.3-1.5%), resilience (40.2-54.7 N.s) and adhesiveness (0.29-0.4 N.s) than the control (250.3 N, 627.9 N, 2.14%, 160.7 N.s, 0.63 N.s), their springiness (0.92-0.93%) was higher than the control (0.79%). Moreover, the color indexes showed that the samples containing PSO in the encapsulated form changed the color indexes more than the control, which was more in the presence of TEO.

Keywords: Encapsulated, Jelly candy, Nanogel, Physicomechanical and structural properties, Pomegranate seed oil, Thyme essential oil

Introduction

In recent years, food consumers are interested in foods that, in addition to having essential nutrients, can improve health, and prevent illnesses as well. Therefore, in Europe and the US, the rate of growth in the production and consumption of fortified foods is increasing (Dias *et al*., 2015). Pomegranate, scientifically named *Punica granatum*, is a fruit with a high concentration of polyphenols compared to other fruits. In addition, pomegranate seed oil (PSO) is one of six known vegetable oils rich in conjugated linolenic fatty acid (CLnA) isomers, which are recommended for preventing from cancer, obesity, diabetes and heart disease. It should be noted that the addition of valuable oils such as pomegranate seed oil to foods has many challenges including their poor dispersion because of low water solubility of these oils as well as their oxidation and creating unfavorable flavors due to their high susceptibility to oxidation in processing and storage conditions (Soleimanian *et al*., 2018; Yekdane and Goli, 2019). Encapsulation and the use of natural or synthetic antioxidants are considered as effective ways to overcome the former and the latter challenges, respectively (Balasubramani *et al.*, 2013). One of the most common methods for encapsulating and delivering bioactive compounds such as pomegranate seed oil in the food and pharmaceutical industries is the use of emulsions (Lamba *et al.*, 2015). Pickering emulsion is an emulsion of any kind, oil-in-water (O/W) or water-in-oil (W/O), or even is multiple that stabilized by solid particles

1- Assistant Professor, School of Agricultural Engineering, Shahrood University of Technology, Shahrood, Iran
(*- Corresponding Author Email: hosseinsg@yahoo.com)
DOI: 10.22067/jam.v11i1.84882

(Jiang *et al.*, 2019). In Pickering emulsions, the particles tend to be irreversibly absorbed at the droplet surface, which creates a physical barrier against prooxidant. Other benefit of Pickering is high resistance to coagulation (McClements and Li, 2010). Nanotechnology has introduced a major revolution in industry, agriculture and other sciences, and draws a very broad perspective to future for the advancement of science. This technology has created many capabilities in postharvest processes of agriculture products (Mirzaee Moghaddam *et al*., 2014). In the past decade, a wide range of polysaccharide nanoparticles have been investigated for the encapsulation of bioactive compounds. Among the different polysaccharides, chitosan (CS), which is produced by deacetylation of chitin, has been used frequently in recent years due to its high biocompatibility. Much research has been done in recent years on Pickering emulsions stabilized by CS (Mwangi *et al.*, 2016; Wang *et al*., 2015). Previous studies have reported that modifying the structure of CS with fatty acids can increase the emulsifier property of CS (Atarian *et al.*, 2019; Hosseini *et al.*, 2019). Thyme with scientific name *Thymus vulgaris* is an aromatic plant of Lamiaceae family and has been considered as a medicinal plant worldwide. According to researchers, the main pharmacological effects of thyme essential oil (TEO) are due to thymol and carvacrol that are the most important bioactive constituents of this plant (Pesavento *et al*., 2015). Essential oils often have antibacterial, antifungal, antiviral and antioxidant properties (Rodríguez *et al*., 2011). However, previous studies have shown that the essential oils, in addition to the properties mentioned, can contribute to the emulsifying activity. Chen *et al.* showed that the combination of cinnamaldehyde, which is a hydrophobic aromatic aldehyde, with CS can increase the emulsifier properties of CS (Chen *et al*., 2017). Developing new foods enriched with bioactive compounds is an interesting marketing strategy for the industry, especially for products such as jelly candy that need to be merged with health revisions. This product is consumed by a large and heterogeneous group of people from children to adults. For this reason, jelly candy can be a good means of delivering bioactive compounds such as PSO to the diet of people (Moura *et al*., 2019).

Previous studies on the production of Pickering emulsions using CS as well as characterization of manufactured emulsions have been performed. However, there has been no study on the encapsulation of PSO using CS nanoparticles containing TEO as well as the effect of the encapsulated PSO on the physicomechanical and structural properties of jelly candy. It should be noted that a proper understanding of the physicochemical and textural properties of new formulations can lead to better design of the devices required for the process of these new formulations on an industrial scale. Therefore, the aim of this study was to investigate the effect of encapsulated PSO by CS-CA nanogel incoporating TEO on the physicomechanical and textural properties of jelly candy.

Materials and Methods

Materials

PSO with 54% punicic acid from "Oil Seed" Company (Iran-Karaj), TEO from "Barijan Essence" (Iran-Kashan), the major constituents of which were included: Thymol (38.5%), Carvacrol (35.1%), Para-cement (8.8%), Gamma-terpene (2.5%) and Beta-caryophyllene (2.2%), CS (90% deacetylated, 50-190 KDa), CA, 1- Ethyl-3- (3-dimethylamino propyl) carbodiimide, acetic acid, sodium hydroxide, ethanol, Nile red and fluorescein isothiocyanate (FITC) from Sigma-Aldrich (Germany), gelatin from "Ghazvin Gelatin Halal" company (Iran-Ghazvin), and liquid glucose from "Orumiyeh Chi Chest Glucose" (Iran- Orumiyeh) were obtained.

Preparation of CS-CA nanogels

CS-CA nanogels were prepared by creating amide bonds between amine groups of CS and carboxylic acid groups of CA with an EDC-mediated reaction (Atarian *et al*., 2019). In brief, 1 g of CS was first dissolved in 100 ml of 1% (v/v) aqueous acetic acid. Then 100 mg EDC was mixed with 500 mg CA and dissolved in 5 ml ethanol subsequently the

mixture of EDC and CA dropwise added to the CS solution and shaked for 24 h at a dark place. In continue, pH of the solution was adjusted on 8.5-9.5 with 1M NaOH and centrifuged for 5 min at 4000 rpm to precipitate the CS-CA gels. After that, to remove unreacted substances and EDC, the precipitated CS-CA gels were washed three times with ethanol and distilled water. Finally, the CS-CA gels were dissolved in aqueous acetic acid 1% (v/v) and sonicated (5 min, 20 kHz) using a probe type ultrasound (Behin Tamin Ahura, Iran) to obtain the CS-CA nanogels and subsequently filtered through a 0.2 µm filter to uniform the CS-CA nanogels in terms of particle size.

Physicochemical and structural characterization of CS-CA nanogels

Fourier transformation infrared (FTIR) spectrometry analysis

To confirm the created amide bonde between CS and CA, an FT/IR-430 Fourier transform infrared spectrometer was used at 20 °C in the range of 500 to 4000 cm^{-1}. Before the analysis, the dried CS-CA nanogels along with the pure CS and CA were mixed with KBr powder subsequently prepared compressed tablets from them (Atarian *et al.*, 2019). In addition, place of testing was in Iran Polymer and Petrochemical Institute.

Scanning electron microscopy (SEM) analysis

The SEM was used to study the morphology of CS-CA nanogels. For this purpose, one droplet of the nanogel solution was first poured on the glassy lam and dried at ambient temperature. In the following, the samples were coated with gold and analyzied using the SEM (model KYKY-EM 3200, Made in China) (Hosseini *et al.*, 2019).

Preparation of PSO-in-water Pickering emulsions

PSO-in-water Pickering emulsions were prepared according to the method of Atarian *et al.* (2019) with some modification. Overall, 20 g PSO was first added dropwise to the CS-CA nanogel solution (2% w/v) and the solution of encapsulated TEO in the CS-CA nanogels (TEO: CS-CA nanogel ratio of 1:4), latter was prepared by the method of Hadian *et al.* (2017), under agitation (600 rppm) with a magnetic stirrer. Then, for better homogeneity of the emulsion, the initial emulsions were homogenized at 8000 rpm (IKA T10 basic, IKA Werke GmbH and Co., Germany) for 2 min. Finally, the solution was sonicated using a probe ultrasound (Behin Tamin Ahura, Iran) for 2 min (on- and off-time pulse durations of 10 and 5 s, respectively), with the power of 600 W, and frequency of 20 kHz.

Average size of droplets

To measure the size of the oil droplets, after 30 minutes of emulsion preparation, one drop of emulsion samples was first taken and gently poured on a glassy lam. Then the image of oil droplets was taken using a GX optical microscope (Australia) equipped with a CCD camera (CM TCAM3). Finally, ImageJ 1.52a software was used to measure the mean of droplets size (Xiao *et al.*, 2016).

Confocal Laser Scanning Microscope (CLSM)

Confocal laser scanning microscope (Heidelberg, Germany) was used to better visualize the interface structure of oil droplets. Prior to emulsion preparation, the CS-CA nanogels were first reacted with FITC (Hosseini *et al.*, 2019). Subsequently, Pickering emulsion was prepared according the method mentioned in section of 2.4 using the CS-CA nanogels bonded to FITC and PSO stained with Nile red. In the following, one droplet of the stained emulsion was poured on a glassy lam. Finally, to obtain photos the laser argon fluorescents at 532 nm for Nile red and 488 nm for FITC were used (Place of testing in Sharif University of Technology).

Preparation of jelly candies

For preparing the different jelly candies, a candy-based mixture formulation consisted of 20% gelatin, 50% distilled water, 10% sugar, and 20% liquid glucose was first perpared in a laboratory water bath at 70 °C. Then, according to Table 1, the certain amount of PSO, TEO, CS-CA nanogel and encapsulated PSO were added to the specified candy-based mixture and blended for 2 min to prepare a unifom mixture. After that, imidiately, the mixtures were moulded into a silicone mould (80×20×50 mm) and kept for 1h in a fridge at 4°C. The jelly candies were then unmoulded

and kept for two days at ambient temperature in a desiccator containing saturated potassium carbonate solution (Mohsenabadi *et al.*, 2018). Finally, the jelly candies were placed in plastic bags and stored at +4°C.

Table 1- Different compounds of the jelly candies

Sample	TEO (%)	Distilled water (%)	CS-CA nanogel (%)	PSO (%)	Blended* (%)
Control	0	10	0	0	90
2% PSO	0	8	0	2	90
2% PSO + 0.1% nanogel	0	7.9	0.1	2	90
2% PSO + 0.1% nanogel+0.05% TEO	0.05	7.85	0.1	2	90
0.1% nanogel	0	9.9	0.1	0	90
0.05% TEO	0.05	9.95	0	0	90

* Glucose (20%) + Gelatin (20%) + Sugar (10%) + Distilled water (50%)

Physicomechanical and structural properties of jelly candies

Microscopic structure

To study the effect of storage on the microstructure of different jelly candies, firstly, 3 and 48 h after preparing the samples, a thin layer from each sample was prepared and, then, analyzed with a GX optical microscope (Australia) equipped with a CCD camera (CM TCAM3).

Physicomechanical properties

Texture Profile Analysis (TPA)

In this study, the texture profile analysis (TPA) of jelly candies was carried out using a Material testing machine (Universal Test Machine, model STM-20, santam Company, Iran). For this purpose, first, from each sample a piece with the dimensions of 20×10×10 mm was prepared. Then, the samples were analyzed with two cycles of loading and unloading, using a cylindrical probe with diameter of 60 mm, speed of 60 mm min^{-1} and displacement length's 80% of the initial height. Finally, the time-force curves for each sample was plotted, and by using these curves (Figure 1), the texture properties namely hardness, cohesiveness, springiness, resilience, adhesiveness, and gumminess determined (Caine *et al.*, 2003). It should note that six replications were considered for each treatment.

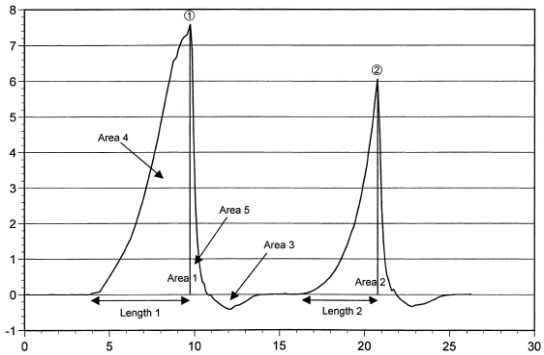

Fig.1. Typical force-by-time plot through two cycles of penetration to determin texture profile analysis parameters. Peak force is hardness; cohesiveness= Area2/Area1; springiness=Length2/Length1; resilience= (Area1-Area2)/2; gumminess= Hardness×cohesiveness; adhesiveness= Area 3 (Caine *et al.*, 2003).

Color evaluation

In order to measure the color indices of difftent jelly candies, three pieces were first selected from each treatment randomly and each piece separately analyzed using a colorimeter (Minoltachroma meter CR-400 KON, Japan, illuminant D_{65}, observer angle 0°). The colorimeter was calibrated with a

white standard plate. The color indices obtained from the colorimeter were L*, a* and b* that respectively represent brightness, redness and yellowness. Finally according to the equations (1), (2) and (3), chroma (color concentration), hue angle (color intensity) and total color difference (ΔE) were calculated for each sample, respectively (Mirzaee Moghaddam *et al*., 2014).

$$C^* = \sqrt{(a^*)^2 + (b^*)^2} \quad (1)$$

$$H^o = ArcTan(\frac{b^*}{a^*}) \quad (2)$$

$$\Delta E = \sqrt{(L_0 - L^*)^2 + (a_0 - a^*)^2 + (b_0 - b^*)^2} \quad (3)$$

Statistical analysis

All experiments except for SEM, CLSM and FTIR were performed in at least three replications. Mean and standard deviation (SD) were calculated using Microsoft Excel 2016 software. One-way ANOVA and Duncan's Multiple Range Test were used to compare differences at the 5% level with SPSS 21 software.

Results and Discussion

Characterization of CS-CA nanogels

FTIR analysis

In the first step of this study, the nanogels were prepared by self-assemble method using modified CS with CA. In order to modify of the CS, some of the free amine groups of CS were attached to the carboxylic acid groups of capric acid by using the EDC intermediate. The spectrums obtained by the FT-IR spectrometer were used to confirm the connection between the CS and CA. Figure 2 shows the FT-IR spectrums of CS, CA and CS-CA nanogel. From Figure 2-a related to CS, a peak in the 3400-3500 cm^{-1} range, which related to the hydroxyl groups of CS, is observed. In addition, at 2875 cm^{-1}, the peak is related to the stretching vibration of the CH_2 bands. At 2137 and 11656 cm^{-1}, the peaks corresponding to the stretching vibrations of the N-C and N-H groups of CS amide (non-acetylated amine groups) are observed, respectively. Moreover, the peak at 1454 cm^{-1} is related to the C-H vibrations in the sugar rings (Hadian *et al.*, 2017; Sabaa *et al.*, 2015). Figure 2-b displays the spectrum of CA that the peaks at 2918 and 2849 cm^{-1} are related to the C-H stretching vibrations of the CH_2 groups. In addition, the peak at 1704 cm^{-1} is related to the C=O stretching vibration of the carboxylic acid group. Moreover, the peak at 1476 cm^{-1} is related to the C-H bending vibration of the CH_2 and CH_3 groups. The peaks at 936 and 687 cm^{-1} are also related to the O-H and C-H bending vibration of the carboxylic acid groups, respectively (Larkin, 2011). Figure 2-c shows the spectrum of CS-CA nanogel. The peak at region 1629 cm^{-1} is due to the vibrations of the amide groups of the acetylated amines (Rao *et al.*, 2012) as well as the new amide bonds formed by the coupling between CS and CA. The peak at region 1527 cm^{-1} is related to the N-H vibration of the second type amide group (Wang *et al.*, 2003), which may be due to the formation of amide bonds between CS and CA. In the nanogel spectrum, a peak is seen in region 1704, which also is seen in the CA spectrum (related to C=O stretching vibration). This peak indicates that a number of carboxylic acid groups of CA have been bonded to the CS chain by electrostatic interactions. These findings are in agreement with the results reported in previous studies (Atarian *et al*., 2019; Hosseini *et al*., 2019).

SEM analysis

Figure 3-a shows the SEM image of CS-CA nanogels. As can be seen in Figure 3-a, the CS-CA filaments had been able to create the particles of about 100 nm by the aggregation. The formation of relatively spherical particles by the CS-CA filaments was probably due to the increasing of hydrophobic property of the CS chains, which caused the hydrophobic parts toward center, and hydrophilic parts toward outside have been arranged and aggregated. These results are consistent with the findings of the other researchers (Atarian *et al*., 2019; Hadian *et al*., 2017; Hosseini *et al*., 2019; Rajaei *et al.*, 2017).

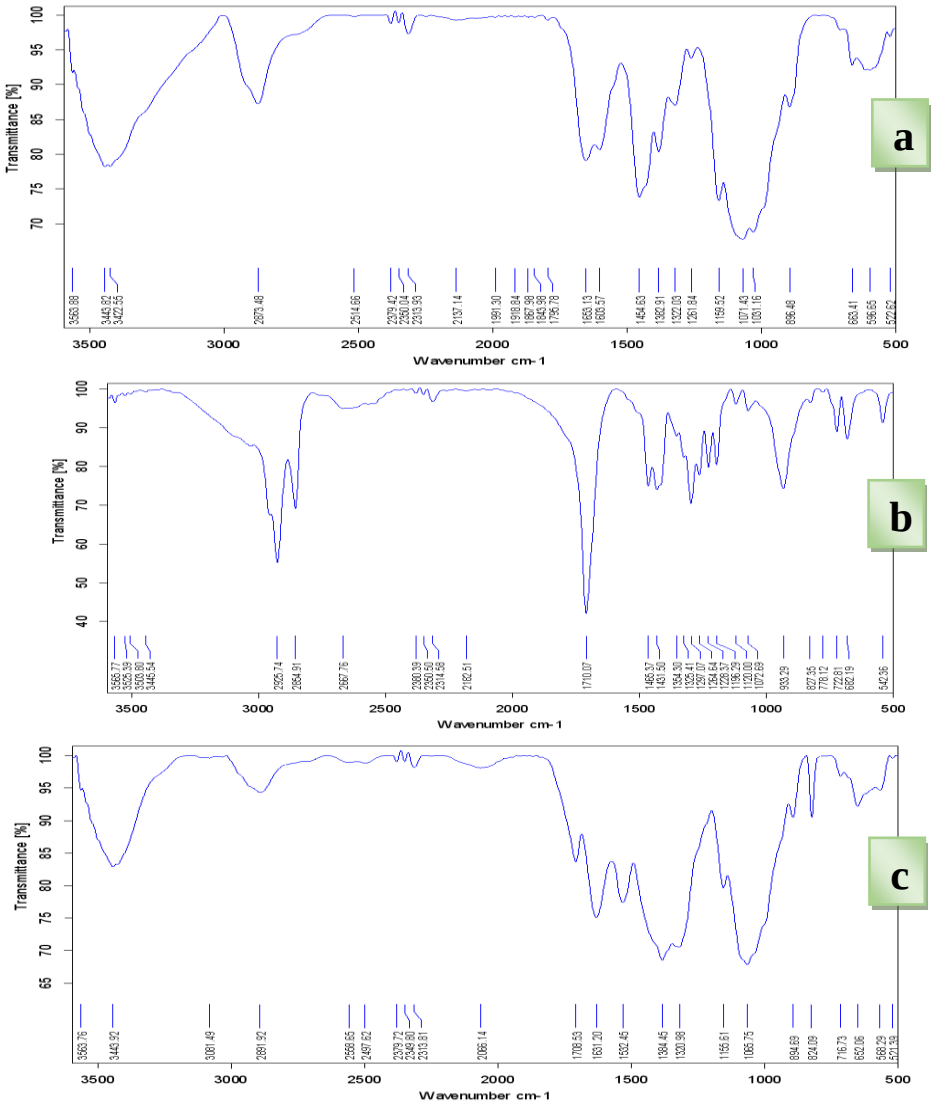

Fig.2. Fourier transform infrared spectroscopy (FTIR) analysis obtained for CS (a), CA (b) and CS-CA nanogel (c)

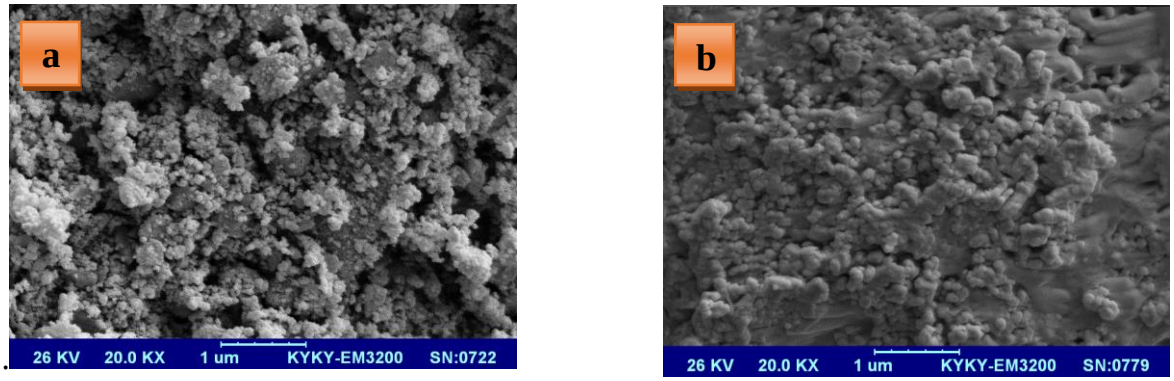

Fig.3. Scanning electron microscopy (SEM) images of CS-CA nanogel (a), and CS-CA nanogel incorporating TEO (b)

To investigate the effect of TEO on the particle size and the shape of CS-CA nanogels, the SEM image was taken from TEO encapsulated with the CS-CA nanogels (Figure 3-b). By comparing the images of CS-CA nanogels and the TEO encapsulated with the nanogels, it can be seen that although the particles are in the range of 100 nm in both figures, the uniformity of particle size distribution is less in the case of TEO encapsulated in the nanogels. Also in the case of the encapsulated TEO, the particles became more interconnected and slightly larger. These results indicate that the encapsulation of TEO in the CS-CA nanogels can change the shape of the particles. This restructuring is probably due to the change in the hydrophilic and the hydrophobic property of the nanogels. Ziaee, *et al.* (2014) investigated the effect of cumin essential oil (2 and 6%) on the size of nanogels. Their results indicated that an increase in the proportion of essential oil loaded in the nanogels maked to create particles of 30 to 250 nm size. In fact, the particle size of nanogels increased with increasing cumin essential oil that was in line with the present results.

Emulsion droplet size

Given that the size of oil droplets can affect the physical properties of jelly candies. In the next step, the CS-CA nanogels alone as well as with TEO was used for stabilizing of PSO-in-water Pickering emulsion, and subsequently the droplet size of emulsions determined. Fig. 4 illustrates the average droplet size as well as the optical microscopic image of Pickering emulsions stabilized with the CS-CA nanogels and the CS-CA nanogels incorporating TEO.

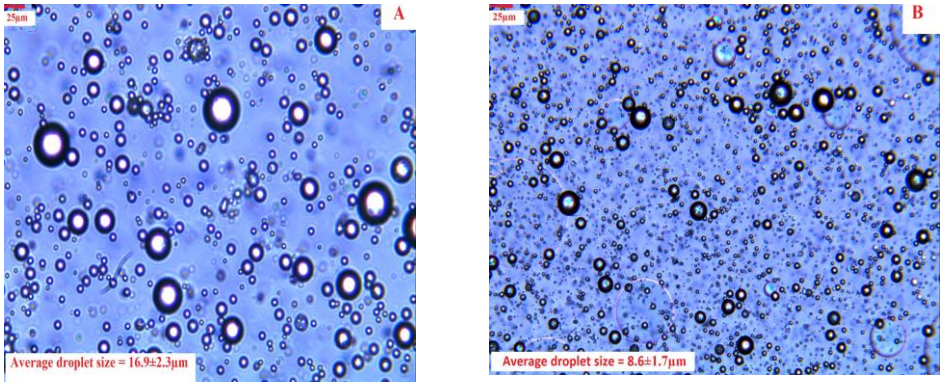

Fig.4. Average droplets size and optical microscopic images of the PSO-in-water Pickering emulsions stabilized by CS-CA nanogel (A), and CS-CA nanogel incorporating TEO (B)

It can be seen from Figure 4 that the average droplet size of emulsion stabilized with the CS-CA nanogels incorporating TEO (Figure 4-B) was smaller than the droplet size of emulsion stabilized with the CS-CA nanogels (Figure 4-A). Due to the hydrophobic nature of TEO, it can be deduced that TEO increased the hydrophobic property of CS-CA nanogels and thus smaller droplets was achieved. These results indicate that the use of TEO incorporating polysaccharides such as CS, whose hydrophilic nature is more than their hydrophobicity, can increase the hydrophobic nature and consequently their emulsifying property. These results are in line with the findings of Chen *et al.* (2017) who reported that cinnamaldehyde in combination with CS could improve the CS emulsifier property.

Interfacial structure

Because the morphological structure of Pickering emulsions including interfacial properties (composition and thickness) affect physical stability, CLSM was used to show the interfacial structure of Pickering emulsion prepared with the CS-CA nanogels that the obtained photos are shown in Figure 5. The CS-CA nanogels and the oil phase were stained by FITC and Nile red, respectively; Thus in Figure 5 the green (A) and red (B) colors represent the nanogels and the oil phase, respectively. Figure 5-C is the combined

fluorescence images of A and B. As shown in Figure 5, the oil phase is located inside the droplets. In addition, the CS-CA nanogels have formed a layer on the surface of droplets, which can create a barrier against coalescence. Moreover, it can be seen that the CS-CA nanogels have formed a dense and continuous network between the oil droplets. Hence, it can be said that in this type of Pickering emulsion, the steric barrier is not a single layer, but rather a network of particles adsorbed on the surface between the oil and the water that causes the steric barrier. The findings of this study, are consistent with those of others (Wang *et al*., 2015; Wongkongkatep *et al*., 2012).

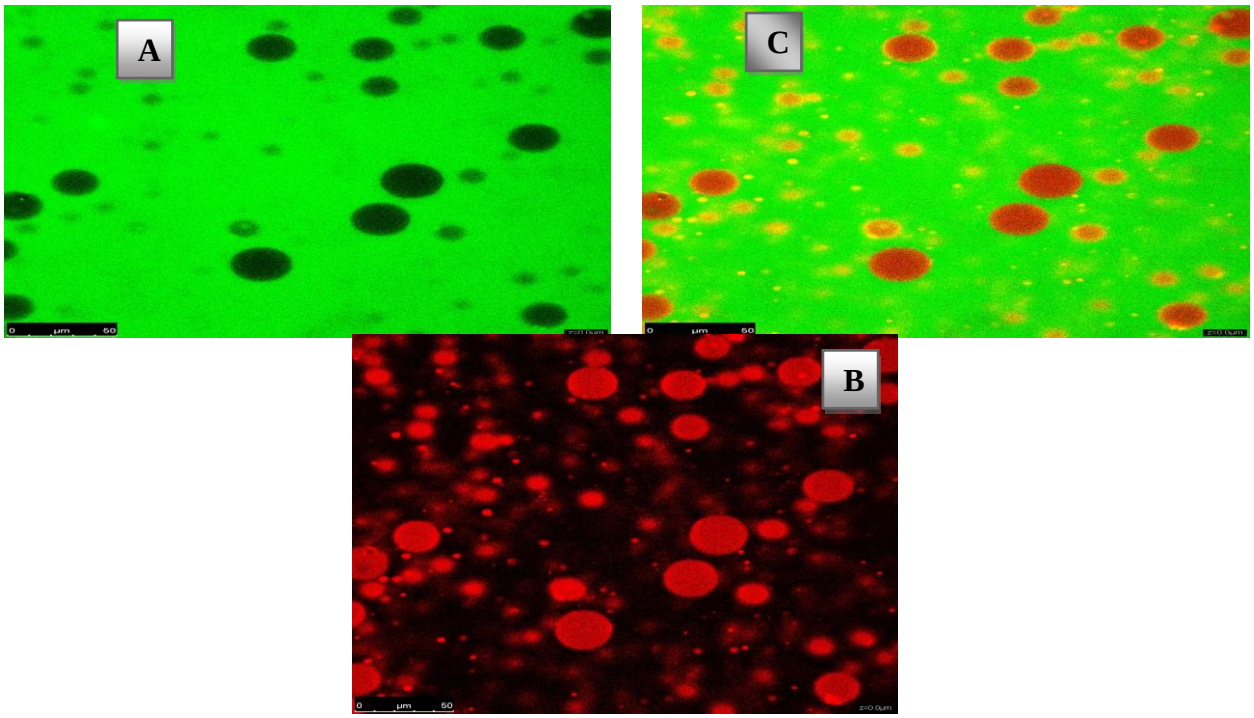

Fig.5. CLSM images of the CS-CA nanogels-stabilized Pickering emulsions: CS-CA nanogels was stained by FITC (green) excited at 488 nm (A); PSO was stained with Nile Red (red) excited at 488 nm (B); combined image of A and B (C)

Physical and mechanical properties of jelly candies enriched with PSO

Microscopic structure of jelly candies

In order to investigate the distribution of PSO droplets, the photo from the surface of samples was taken by the optical microscope. Figure 6 shows the optical microscope images obtained from the surface of different samples after 3 and 48 h of storage. According to Figure 6, it can be seen that among the control, the jelly candy containing 2% nanogel as well as the jelly candy incoporating 2% nanogel+ 0.05% TEO was not observed any significant difference in their structure after 48 h of storage. About the samples containing 2% PSO+0.1% nanogel and 2% PSO+0.1% nanogel+0.05% TEO after 48 h, was observed slightly larger droplets and drops accumulation in some spots. In addition, in the case of the sample containing 2% PSO+0.1% nanogel+0.05% TEO, the oil droplets were slightly smaller than the sample containing 2% PSO+0.1% nanogel. From Figure 6, the highest change in texture was observed in the samples containing 2% PSO compared to the other samples. About jelly candy with 2% PSO, the large droplets of PSO were observed in the matrix of sample after 3 h of storage. However, after 48 h of storage, the PSO droplets were completely separated from the jelly candy matrix and accumulated on its surface (Figure 6). The reason for the

separation of oil from the sample matrix with 2% PSO can be attributed to the lack of using of stabilizer. This result clearly showed that the use of PSO in the form of emulsion stabilized by the CS-CA nanogels was able to contribute to better dispersion and physical stability of oil droplets during storage.

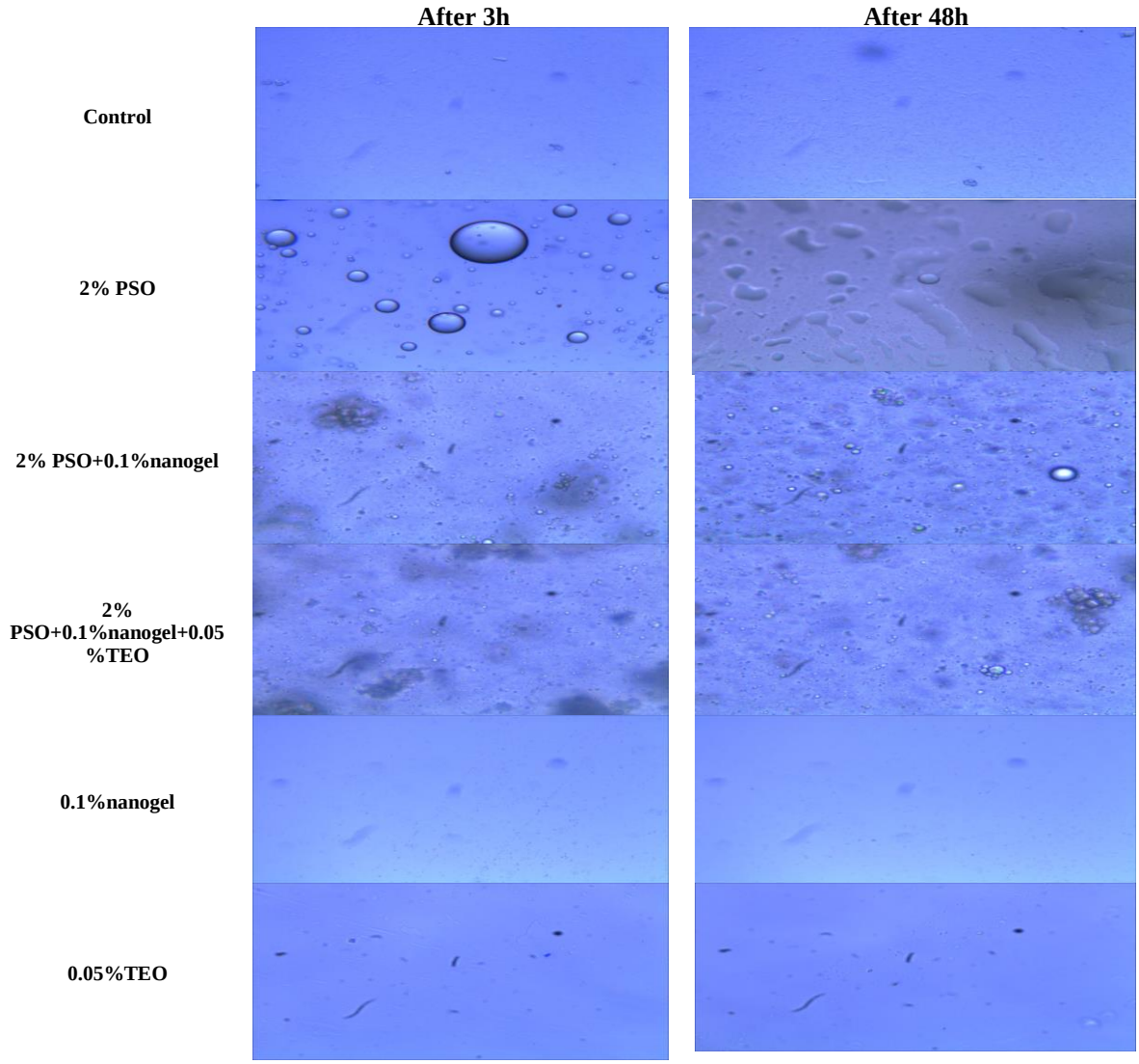

Fig.6. Surface microscopic images of different jelly candy samples

Texture profile analysis (TPA)

Figure 7 displays the results of TPA (hardness, cohesiveness, springiness, resilience, adhesiveness and gumminess) for the different jelly candy samples. As shown in Figure 7-a, it can be seen that the hardness of the control was higher than of all. Whereas the hardness of the jelly candies decreased by adding of PSO and TEO. In the case of jelly candies containing only 0.1% nanogel, the hardness results showed that the effect of the nanogel alone did not have a significant ($p>0.05$) effect on the hardness. From Figure 7-b, the results showed that the cohesiveness property of the control was higher than the rest of the samples, with a significant difference at 5% level. It should be noted that the cohesiveness property reflects the strength of intermolecular interactions. These results showed that the PSO, CS-CA nanogels, and TEO could attenuate the intermolecular forces of the candy structure. Concerning the results

of springiness, it can be seen that the adding of CS-CA nanogel, TEO and PSO to the jelly candy structure significantly ($p\leq0.05$) increased the springiness compared to the control sample. Moreover, the CS-CA nanogels had the most effect on increasing the springiness property (Figure 7-c). Regarding the resilience, the highest resilience was observed in the control sample, which was significantly different ($p\leq0.05$) from the other samples (Figure 7-d). The results of adhesiveness property showed that the use of PSO as well as nanogels reduced the adhesiveness of the samples compared to the control sample (Figure 7-e). Regarding the gumminess property, the highest gumminess belonged to the control sample, which had a significant difference at 5% level with the other samples. Results of gumminess property showed that the use of nanogel, PSO and TEO reduced this property (Figure 7-f). The observed trend in gumminess property was approximately similar to the hardness and resilience properties. The trend similarity of these properties is probably due to their high correlation. Various works have been done on the enrichment of jelly candy and the effect of enriching compounds on the mechanical properties of jelly candy. For example, Hani *et al.* (2015) reported that the red pitaya fruit puree in the formulation of gummy candy decresed the hardness and gumminess of gummy candy. Amjadi *et al.* (2018) also stated that increasing the amount of betanin in the gummy candy structure reduced its hardness and gumminess properties. In addition, Mogaddas Kia *et al.* (2020) showed that the red beet extract in the gummy candy formulation reduced the gumminess property. They interpreted that this gumminess reduction due the presence of red beet extract may be related to induce heterogeneity to network structure. Most research has focused on the effect of CS and gelatin on the mechanical properties of edible films, and no specification research was observed for mechanical properties of jelly candies. For this reason, the researches on edible films that are almost as close to the texture of jelly candy was used to interpret the results. Among these investigations, Benbettaïeb *et al.* (2014) reported that gelatin film had more hardness and less resilience than CS film. The addition of CS to the gelatin film also reduced their hardness and increased their resilience. These researchers reported that more hardness and less resilience of the gelatin films related the denser gelatin-created network. Thus, when the CS was combined with gelatin, due to the interaction between the two polymers, the hydrogen bonds between the gelatin polymers reduced and in fact, CS acted as a plasticizer, which made it more flexible (Benbettaïeb *et al*., 2014). These results are in agreement with the findings regarding the hardness and resilience of the present study. Various studies have been performed on the effect of oil on the texture properties of edible films. For example, Valenzuela *et al*. (2013) reported that the sunflower oil could reduced the strength of CS and protein blend films. These researchers have attributed the decrease of film strength due to the effect of oil on increasing structural heterogeneity and decreasing structure adhesion forces.

Color analysis

The results of color analysis for the different jelly candy samples are shown in Table 2. The results of the brightness index (L*) showed that the use of unencapsulated PSO reduced this index. Nevertheless, using encapsulated PSO (2% PSO+0.1 nanogel and 2% PSO+0.1 nanogel+0.05% TEO) increased the brightness index, which had a significant difference ($p\leq0.05$) with the control sample. A similar trend was observed for the redness index (a*) such as the brightness index. It should be noted that the positive values of a* index are red equivalent and the negative values are green equivalent. These results showed that the PSO in the emulsified form increased the green color of the samples. In the case of b* index, it was observed that the PSO in the form of emulsion, compared to the control sample, reduced this index significantly. In addition, the b* index of jelly candy containing 2% PSO+0.1 nanogel+0.05% TEO was lower than that of

jelly candy containing 2% PSO+0.1 nanogel. The results of total color difference (ΔE) showed that the least ΔE was related to the sample containing 0.1% nanogel and the highest color difference was for the samples containing PSO in emulsified form (2% PSO+0.1 nanogel and 2% PSO+0.1 nanogel+0.05% TEO). It should be noted that the total color differences of less than 3-4, are not detectable by the human eye (Benbettaïeb *et al.*, 2014). The results of color intensity (Hue angle) and color concentration (chroma) also showed that the PSO in the form of emulsion (2% PSO+0.1% nanogel and 2% PSO+0.1% nanogel+0.05% TEO) reduced the both indices. The overall results of color indices showed that the most color changes were in the samples containing PSO in the emulsified form.

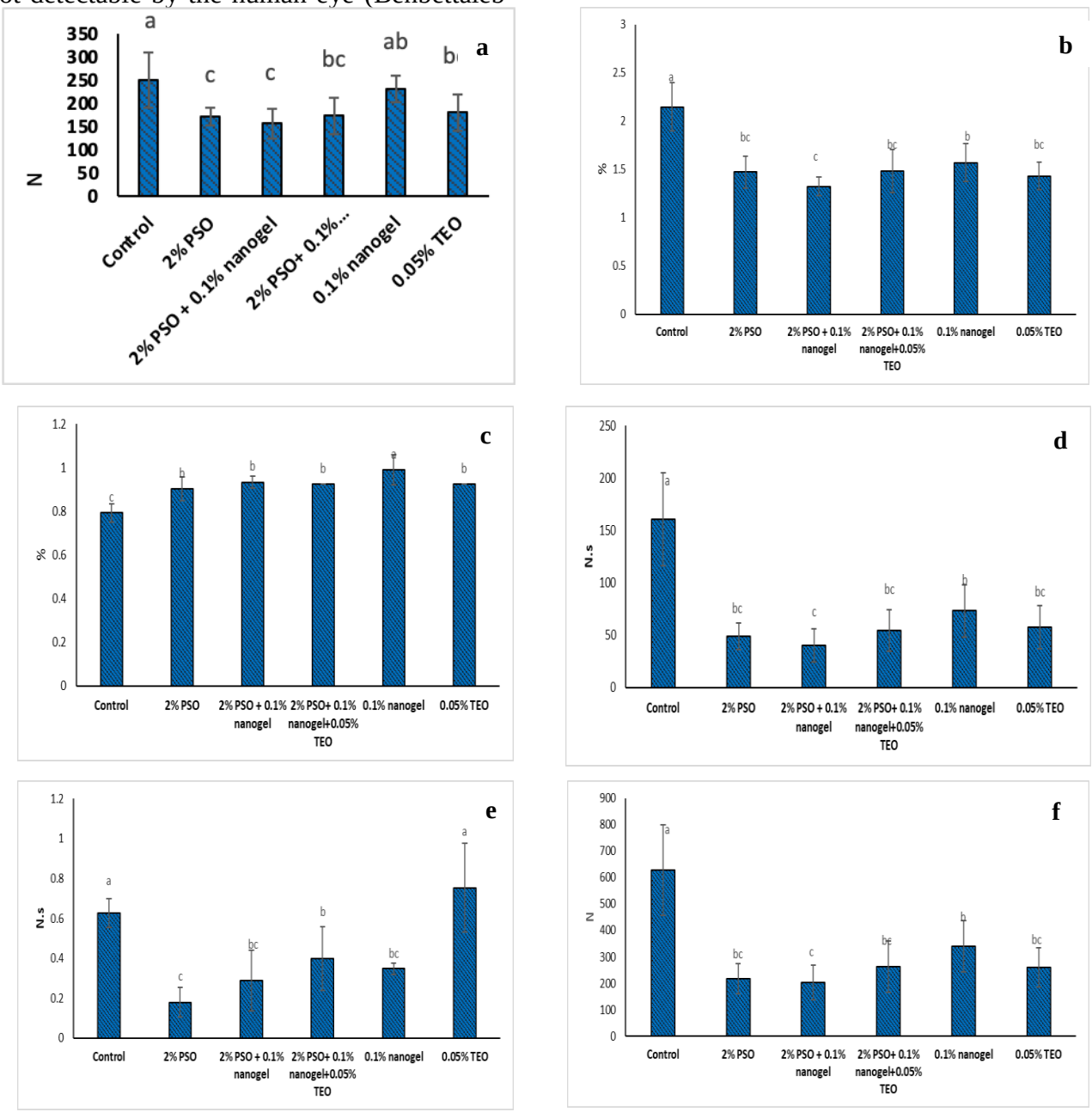

Fig.7. Hardness (a), Cohesiveness (b), Springiness (c), Resilience (d), Adhesiveness (e) and Gumminess (f) of jelly candy samples

Table 2- Color parameters of jelly candies

Treatment	L^*	a^*	b^*	ΔE	Hue Angle	Chroma
Control	52.53±0.76^{cd}	-1.20±0.35^{b}	53.93±0.50^{a}	-	267.48±1.57^{a}	54.00±0.44^{a}
2%PSO	48.07±1.40^{e}	1.40±0.20^{a}	49.53±0.50^{b}	12.52±1.10^{c}	268.38±0.21^{a}	49.55±0.51^{b}
2% PSO + 0.1% nanogel	56.47±1.92^{b}	-7.60±0.92^{d}	33.20±1.22^{b}	19.97±1.02^{b}	102.86±1.08^{c}	34.06±1.38^{c}
2% PSO + 0.1% nanogel+0.05% TEO	60.66±1.96^{a}	-8.47±0.50^{d}	31.40±1.40^{c}	21.93±1.19^{a}	105.08±0.29^{b}	32.52±1.48^{c}
0.1% nanogel	53.53±1.50^{c}	-3.1±0.30^{c}	54.0±0.40^{a}	5.92±1.23^{e}	92.19±1.93^{d}	54.06±0.36^{a}
0.05%TEO	50.40±0.40^{de}	-1.60±0.35^{b}	52.93±0.61^{a}	8.55±0.24^{d}	91.73±0.39^{d}	52.95±0.60^{a}

Values with different letters (a-e) in same column are significantly different, p<0.05.

Figure 8 displays the surface photo of different samples of jelly candy. In Figure 8, the color difference of the samples containing the PSO in emulsified form (2% PSO+0.1% nanogel and 2% PSO+0.1% nanogel+0.05% TEO) with the other samples is clearly seen. The samples containing the PSO in emulsified form had a lighter color than the other samples. The obvious difference between the samples containing PSO in the emulsified form, in terms of color indices, is probably due to the presence of oil droplets in the jelly candies texture. These oil droplets can change the transparency of the samples. The interaction between oil and water molecules also changes the refractive index of hydrocolloid compounds, which can change the color indices (Pereda *et al.*, 2012).

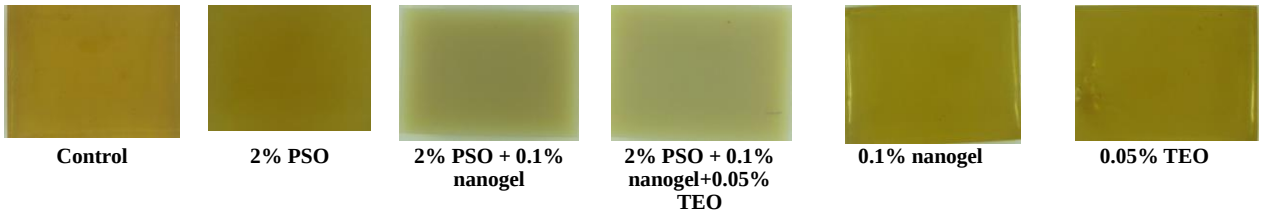

Fig.8. Appearance of different jelly candy samples

Conclusions

In this study, Pickering emulsion method using CS-CA nanogel incorporating TEO as a stabilizer was used to encapsulate PSO and subsequently to enrich jelly candy. The results showed that the use of PSO in the emulsified form improved the dispersion and physical stability of PSO in the jelly candy structure; nevertheless it reduced some of the textural properties such as hardness of jelly candy as well as changed the color characteristics of jelly candy. Physicomechanical results of jelly candy enriched with encapsulated PSO in this study can lead to better design of the devices required for the process of this new formulation on an industrial scale.

References

1. Amjadi, S., M. Ghorbani, H. Hamishehkar, and L. Roufegarinejad. 2018. Improvement in the stability of betanin by liposomal nanocarriers: Its application in gummy candy as a food model. Food Chemistry 256: 156-162.
2. Atarian, M., A. Rajaei, M. Tabatabaei, A. Mohsenifar, and H. Bodaghi. 2019. Formulation of Pickering sunflower oil-in-water emulsion stabilized by chitosan-stearic acid nanogel and studying its oxidative stability. Carbohydrate Polymers 210: 47-55.
3. Aveyard, R., B. P. Binks, and J. H. Clint. 2003. Emulsions stabilised solely by colloidal particles. Advances in Colloid and Interface Science 100: 503-546.
4. Balasubramani, P., R. Viswanathan, and M. Vairamani. 2013. Response surface optimisation of process variables for microencapsulation of garlic (*Allium sativum* L.) oleoresin by spray drying. Biosystems Engineering 114 (3): 205-213.

5. Benbettaieb, N., M. Kurek, S. Bornaz, and F. Debeaufort. 2014. Barrier, structural and mechanical properties of bovine gelatin-chitosan blend films related to biopolymer interactions. Journal of the Science of Food and Agriculture 94 (12): 2409-2419.
6. Beyki, M., S. Zhaveh, S. T. Khalili, T. Rahmani-Cherati, A. Abollahi, M. Bayat, and A. Mohsenifar. 2014. Encapsulation of Mentha piperita essential oils in chitosan–cinnamic acid nanogel with enhanced antimicrobial activity against Aspergillus flavus. Industrial Crops and Products 54: 310-319. https://doi.org/http://dx.doi.org/10.1016/j.indcrop.2014.01.033
7. Caine, W. R., J. L. Aalhus, D. R. Best, M. E. R. Dugan, and L. E. Jeremiah. 2003. Relationship of texture profile analysis and Warner-Bratzler shear force with sensory characteristics of beef rib steaks. Meat Science 64 (4): 333-339.
8. Chen, H., D. J. McClements, E. Chen, S. Liu, B. Li, and Y. Li. 2017. In situ interfacial conjugation of chitosan with cinnamaldehyde during homogenization improves the formation and stability of chitosan-stabilized emulsions. Langmuir 33 (51): 14608-14617.
9. de Moura, S. C. S. R., C. L. Berling, A. O. Garcia, M. B. Queiroz, I. D. Alvim, and M. D. Hubinger. 2019. Release of anthocyanins from the hibiscus extract encapsulated by ionic gelation and application of microparticles in jelly candy. Food Research International 121: 542-552.
10. Dias, M. I., I. C. F. R. Ferreira, and M. F. Barreiro. 2015. Microencapsulation of bioactives for food applications. Food & Function 6 (4): 1035-1052.
11. Golmakani, M. T., and K. Rezaei. 2008. Comparison of microwave-assisted hydrodistillation withthe traditional hydrodistillation method in the extractionof essential oils from *Thymus vulgaris* L. Food Chemistry 109 (4): 925-930.
12. Hadian, M., A. Rajaei, A. Mohsenifar, and M. Tabatabaei. 2017. Encapsulation of Rosmarinus officinalis essential oils in chitosan-benzoic acid nanogel with enhanced antibacterial activity in beef cutlet against Salmonella typhimurium during refrigerated storage. LWT-Food Science and Technology 84: 394-401.
13. Hani, N. M., S. R. Romli, and M. Ahmad. 2015. Influences of red pitaya fruit puree and gelling agents on the physico-mechanical properties and quality changes of gummy confections. International Journal of Food Science & Technology 50 (2): 331-339.
14. Hosseini, E., A. Rajaei, M. Tabatabaei, A. Mohsenifar, and K. Jahanbin. 2019. Preparation of Pickering Flaxseed Oil-in-Water Emulsion Stabilized by Chitosan-Myristic Acid Nanogels and Investigation of Its Oxidative Stability in Presence of Clove Essential Oil as Antioxidant. Food Biophysics 1-13.
15. Jiang, Y., F. Li, D. Li, D. Sun-Waterhouse, and Q. Huang. 2019. Zein/Pectin Nanoparticle-Stabilized Sesame Oil Pickering Emulsions: Sustainable Bioactive Carriers and Healthy Alternatives to Sesame Paste. Food and Bioprocess Technology 1-11.
16. Kakran, M., and M. N. Antipina. 2014. Emulsion-based techniques for encapsulation in biomedicine, food and personal care. Current Opinion in Pharmacology 18: 47-55.
17. Lamba, H., K. Sathish, and L. Sabikhi. 2015. Double emulsions: emerging delivery system for plant bioactives. Food and Bioprocess Technology 8 (4): 709-728.
18. Larkin, P. 2011. Infrared and Raman spectroscopy: principles and spectral interpretation. Elsevier.
19. McClements, D. J. 2010. Emulsion design to improve the delivery of functional lipophilic components. Annual Review of Food Science and Technology 1: 241-269.
20. McClements, D. J., and Y. Li. 2010. Structured emulsion-based delivery systems: Controlling the digestion and release of lipophilic food components. Advances in Colloid and Interface Science 159 (2): 213-228.
21. Moghaddas Kia, E., S. Ghaderzadeh, A. M. Langroodi, Z. Ghasempour, and A. Ehsani. 2020. Red beet extract usage in gelatin/gellan based gummy candy formulation introducing Salix

aegyptiaca distillate as a flavouring agent. Journal of Food Science and Technology https://doi.org/10.1007/s13197-020-04368-8
22. Mohsenabadi, N., A. Rajaei, M. Tabatabaei, and A. Mohsenifar. 2018. Physical and antimicrobial properties of starch-carboxy methyl cellulose film containing rosemary essential oils encapsulated in chitosan nanogel. International Journal of Biological Macromolecules 112: 148-155.
23. Mwangi, W. W., K. W. Ho, B. T. Tey, and E. S. Chan. 2016. Effects of environmental factors on the physical stability of pickering-emulsions stabilized by chitosan particles. Food Hydrocolloids 60: 543-550. https://doi.org/10.1016/j.foodhyd.2016.04.023.
24. Pereda, M., G. Amica, and N. E. Marcovich. 2012. Development and characterization of edible chitosan/olive oil emulsion films. Carbohydrate Polymers 87 (2): 1318-1325.
25. Pesavento, G., C. Calonico, A. R. Bilia, M. Barnabei, F. Calesini, R. Addona, and A. Lo Nostro. 2015. Antibacterial activity of Oregano, Rosmarinus and Thymus essential oils against Staphylococcus aureus and Listeria monocytogenes in beef meatballs. Food Control 54: 188-199. https://doi.org/http://dx.doi.org/10.1016/j.foodcont.2015.01.045.
26. Pu, J., J. D. Bankston, S. Sathivel. 2011. Developing microencapsulated flaxseed oil containing shrimp (*Litopenaeus setiferus*) astaxanthin using a pilot scale spray dryer. Biosystems Engineering 108 (2): 121-132.
27. Rajaei, A., M. Hadian, A. Mohsenifar, T. Rahmani-Cherati, M. Tabatabaei. 2017. A coating based on clove essential oils encapsulated by chitosan-myristic acid nanogel efficiently enhanced the shelf-life of beef cutlets. Food Packaging and Shelf Life 14: 137-145.
28. Rao, K. S. V. K., P. R. Reddy, Y. I. Lee, and C. Kim. 2012. Synthesis and characterization of chitosan--PEG--Ag nanocomposites for antimicrobial application. Carbohydrate Polymers 87 (1): 920-925.
29. Rodríguez, F. P., D. Campos, E. T. Ryser, A. L. Buchholz, G. D. Posada-Izquierdo, B. P. Marks, and E. Todd. 2011. A mathematical risk model for Escherichia coli O157: H7 cross-contamination of lettuce during processing. Food Microbiology 28 (4): 694-701.
30. Rota, M. C., A. Herrera, R. M. Mart\'\inez, J. A. Sotomayor, and M. J. Jordán. 2008. Antimicrobial activity and chemical composition of Thymus vulgaris, Thymus zygis and Thymus hyemalis essential oils. Food Control 19 (7): 681-687.
31. Sabaa, M. W., H. M. Abdallah, N. A. Mohamed, and R. R. Mohamed. 2015. Synthesis , Characterization and Application of Biodegradable Crosslinked Carboxymethyl Chitosan / Poly Vinyl. Materials Science & Engineering 56: 363-373. https://doi.org/10.1016/j.msec.2015.06.043.
32. Soleimanian, Y., S. A. H. Goli, J. Varshosaz, and S. M. Sahafi. 2018. Formulation and characterization of novel nanostructured lipid carriers made from beeswax, propolis wax and pomegranate seed oil. Food Chemistry 244: 83-92. https://doi.org/10.1016/j.foodchem.2017.10.010
33. Valenzuela, C., L. Abugoch, and C. Tapia. 2013. Quinoa protein-chitosan-sunflower oil edible film: Mechanical, barrier and structural properties. LWT-Food Science and Technology 50 (2): 531-537.
34. Wang, L. J., Y. Q. Hu, S. W. Yin, X. Q. Yang, F. R. Lai, and S. Q. Wang. 2015. Fabrication and characterization of antioxidant pickering emulsions stabilized by zein/chitosan complex particles (ZCPs). Journal of Agricultural and Food Chemistry 63 (9): 2514-2524. https://doi.org/10.1021/jf505227a.
35. Wang, X. H., D. P. Li, W. J. Wang, Q. L. Feng, F. Z. Cui, Y. X. Xu, M. van der Werf. 2003. Crosslinked collagen/chitosan matrix for artificial livers. Biomaterials 24 (19): 3213-3220.
36. Wei, Z., C. Wang, S. Zou, H. Liu, Z. Tong. 2012. Chitosan nanoparticles as particular emulsifier for preparation of novel pH-responsive Pickering emulsions and PLGA

microcapsules. Polymer 53 (6): 1229-1235. https://doi.org/10.1016/j.polymer.2012.02.015.
37. Wongkongkatep, P., K. Manopwisedjaroen, P. Tiposoth, S. Archakunakorn, T. Pongtharangkul, M. Suphantharika, J. Wongkongkatep. 2012. Bacteria Interface Pickering Emulsions Stabilized by Self-assembled Bacteria–Chitosan Network. Langmuir 28 (13): 5729-5736. https://doi.org/10.1021/la300660x.
38. Xiao, J., X. Wang, A. J. Perez Gonzalez, and Q. Huang. 2016. Kafirin nanoparticles-stabilized Pickering emulsions: Microstructure and rheological behavior. Food Hydrocolloids 54: 30-39. https://doi.org/10.1016/j.foodhyd.2015.09.008.
39. Yekdane, N., and S. A. H. Goli. 2019. Effect of Pomegranate Juice on Characteristics and Oxidative Stability of Microencapsulated Pomegranate Seed Oil Using Spray Drying. Food and Bioprocess Technology 12 (9): 1614-1625.
40. Zhang, S., Y. Zhou, C. Yang. 2015. Pickering emulsions stabilized by the complex of polystyrene particles and chitosan. Colloids and Surfaces A: Physicochemical and Engineering Aspects 482: 338-344.
41. Zhang, Y., L. Yang, Y. Zu, X. Chen, F. Wang, and F. Liu. 2010. Oxidative stability of sunflower oil supplemented with carnosic acid compared with synthetic antioxidants during accelerated storage. Food Chemistry 118 (3): 656-662.
42. Zhaveh, S., A. Mohsenifar, M. Beiki, S. T. Khalili, A. Abdollahi, T. Rahmani-Cherati, and M. Tabatabaei. 2015. Encapsulation of Cuminum cyminum essential oils in chitosan-caffeic acid nanogel with enhanced antimicrobial activity against Aspergillus flavus. Industrial Crops and Products 69: 251-256. https://doi.org/http://dx.doi.org/10.1016/j.indcrop.2015.02.028.
43. Ziaee, M., S. Moharramipour, and A. Mohsenifar. 2014. Toxicity of Carum copticum essential oil-loaded nanogel against Sitophilus granarius and Tribolium confusum. Journal of Applied Entomology 138 (10): 763-771.

نشریه ماشین‌های کشاورزی
جلد ۱۱، شماره ۱، نیمسال اول ۱۴۰۰، ص ۷۰-۵۵

Journal of Agricultural Machinery
Vol. 11, No. 1, Spring- Summer 2021, p. 55-70

مقاله علمی- پژوهشی

تأثیر روغن هسته انار کپسوله شده در نانوژل‌های کیتوزان-کاپریک اسید حاوی اسانس آویشن بر خواص فیزیکومکانیکی و ساختاری آبنبات ژله‌ای

حسین میرزائی مقدم[1*]، احمد رجائی[1]

تاریخ دریافت: ۱۳۹۸/۱۰/۱۱
تاریخ پذیرش: ۱۳۹۹/۰۳/۰۳

چکیده

روغن هسته انار (PSO) منبع شناخته شده‌ای از ترکیبات با ارزش است. بنابراین هدف از این مطالعه بررسی خواص فیزیکومکانیکی و ساختاری آبنبات ژله‌ای غنی شده با روغن هسته انار درون‌پوشانی شده در نانوژل‌های کیتوزان (CS)-کاپریک اسید (CA) حاوی اسانس آویشن (TEO) است. بدین منظور، در ابتدا نانوژل‌های کیتوزان-کاپریک اسید، با ایجاد پیوند آمید بین کیتوزان و کاپریک اسید تولید شدند که تصویر میکروسکوپ الکترونی روبشی (SEM) شکل کروی نانوژل‌های کیتوزان-کاپریک اسید را نشان داد. سپس امولسیون پیکرینگ روغن هسته انار با نانوژل کیتوزان-کاپریک اسید و اسانس آویشن درون‌پوشانی شده در نانوژل کیتوزان-کاپریک اسید پایدار شدند. نتایج نشان داد که حضور اسانس آویشن در ساختار نانوژل باعث ایجاد قطرات روغن کوچک‌تر شد. در ادامه از امولسیون‌های پیکرینگ در فرمولاسیون آبنبات ژله‌ای استفاده شد و متعاقباً ساختار میکروسکوپی، آنالیز بافت (TPA) و شاخص‌های رنگ آبنبات‌های ژله‌ای مورد بررسی قرار گرفت. استفاده از روغن هسته انار به‌صورت درون کپسوله شده، باعث کاهش جدا شدن روغن هسته انار از بافت آبنبات ژله‌ای شد. نتایج آزمون پروفایل بافت نشان داد که اگرچه نمونه‌های حاوی امولسیون روغن هسته انار، سختی (N۱۷۳/۴-۱۵۶/۶)، صمغی بودن (N۲۶۲/۱-۲۰۲/۲)، انسجام (۱/۳-۱/۵٪)، خاصیت ارتجاعی (N.s ۵۴/۷-۴۰/۲) و چسبندگی (N.s ۰/۴-۰/۲۹) کمتری نسبت به نمونه شاهد (N۲۵۰/۳، N۶۲۷/۹، N.s۱۶۰/۷، N.s۰/۶۳) داشتند، خاصیت فنریت آن‌ها (۰/۹۲-۰/۹۳٪) بیشتر از نمونه شاهد (۰/۷۹٪) بود. علاوه بر این، نتایج شاخص‌های رنگی نشان داد که نمونه‌های حاوی روغن هسته انار کپسوله شده باعث تغییر شاخص‌های رنگی نسبت به نمونه شاهد شد که این تغییر در حضور اسانس آویشن بیشتر بود.

واژه‌های کلیدی: آبنبات ژله‌ای، اسانس آویشن، خواص فیزیکومکانیکی و ساختاری، روغن هسته انار، کپسوله شده، نانوژل

۱- استادیار دانشکده کشاورزی، دانشگاه صنعتی شاهرود
(*- نویسنده مسئول: Email: hosseinsg@yahoo.com)

DOI: 10.22067/jam.v11i1.84882